4-cyanopyridine does not depend on its bonding mode.[30]

Finally, it is noteworthy that the activation parameters for intramolecular electron transfer in VII, $\Delta H^{\ddagger} = 23.4 \pm 0.5$ kcal/mol and $\Delta S^{\ddagger} = 19.2 \pm 0.2$ cal/(deg mol), compare favorably with the values for intramolecular electron transfer in the related systems XVII (24.6 ± 1.4 kcal/mol, 18 ± 5 cal/mol deg)[31] and XVIII (24.5 ± 0.3 kcal/mol, 10.6 ± 1.0 cal/(mol deg)).[5] The

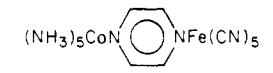

XVII

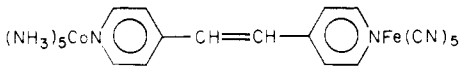

XVIII

sizable positive entropies of activation are to be contrasted with the near-zero values measured for intramolecular electron transfer in *trans*-$(H_2O)(NH_3)_4RuLCo(NH_3)_5^{5+}$ (L = 4,4′-bipyridine, 1,2-bis(4-pyridyl)ethylene, 3,3′-dimethyl-4,4′-bipyridine, bis(4-pyridyl) sulfide).[32] The values of $\Delta S^{\ddagger}$ are rationalized on the basis of the charge redistribution concept.[20] For the iron systems, in going from precursor to successor complex, the charge separation goes from 3+,3- to 2+,2-, whereas for the ruthenium system no change in charge separation obtains upon electron transfer, 3+,2+ being the charge separation in both precursor and successor complexes. For the iron systems, the charge redistribution would be accompanied by a decrease in solvation and, consequently, a positive entropy of activation. For the ruthenium systems, the electron transfer does not change the net charge distribution, no net change in solvation takes place, and consequently, a near-zero entropy of activation obtains.

Registry No. $Fe(CN)_5OH_2^{3-}$, 18497-51-3; $Co(NH_3)_5NC_5H_4CN^{3+}$, 46247-07-8; $Co(NH_3)_5NCC_5H_4N^{3+}$, 53739-10-9; $Co(NH_3)_5$-1,3-$NC_5H_4CN^{3+}$, 80041-64-1; $Co(NH_3)_5NC$-3,1-$C_5H_4N^{3+}$, 53739-14-3; $(NC)_5FeNC_5H_4CNCo(NH_3)_5$, 81095-43-4; $(NC)_5FeNCC_5H_4NCo(NH_3)_5$, 81063-99-2; $(NC)_5Fe$-1,3-$NC_5H_4CNCo(NH_3)_5$, 81064-00-8; $(NC)_5FeNC$-3,1-$C_5H_4NCo(NH_3)_5$, 81064-01-9.

(30) The differences in reduction potentials and self-exchange rates for nitrile-bound and pyridine-bound complexes of $Co(NH_3)_5^{3+}$ and 4-cyanopyridine are assumed to be small. We have no direct information on this point. However, the rates of reduction of nitrile-bound and pyridine-bound complexes of $Co(NH_3)_5^{3+}$ with 3-cyanopyridine differ by a factor of 2: Miralles, A. J.; Szecsy, A. P.; Haim, A. *Inorg. Chem.* **1982**, *21*, 697.

(31) Malin, J. M.; Ryan, D. A.; O'Halloran, T. V. *J. Am. Chem. Soc.* **1978**, *100*, 2097.

(32) Fischer, H.; Tom, G. M.; Taube, H. *J. Am. Chem. Soc.* **1976**, *98*, 5512.

X-ray Structures of Two Unexpected Complexes Isolated during CO Substitutions by Phosphine Ligands in Dinuclear Bridged d^8 Metal Complexes

Philippe Kalck,[1] Jean-Jacques Bonnet, and René Poilblanc*

Contribution from the Laboratoire de Chimie de Coordination du C.N.R.S. associé à l'Université Paul Sabatier, F 31400 Toulouse, France. *Received June 10, 1981*

Abstract: The reaction of $[Ir_2(\mu\text{-S-}t\text{-Bu})_2(CO)_4]$ in concentrated hexane solution with 2 mol of trimethylphosphine results in the two complexes $[Ir_2(\mu\text{-CO})(\mu\text{-S-}t\text{-Bu})(CO)_2(\text{S-}t\text{-Bu})(PMe_3)_3]$ and $[Ir_3(\mu\text{-CO})(\mu\text{-S-}t\text{-Bu})_3(CO)_4(PMe_3)_2]$, for which the structures have been determined by X-ray crystallography. The first complex crystallizes in space group $P\bar{4}2_1c$ with $a = 15.334$ (2) Å, $c = 26.623$ (4) Å, and $Z = 8$. On the basis of 2313 unique reflections, the structure was refined by full-matrix least-squares techniques to conventional indices of $R = 0.045$ and $R_w = 0.035$. The Ir–Ir separation is 2.702 (1) Å, and a CO ligand is in a bridging position whereas a S-*t*-Bu ligand is in an equatorial position. The complex $[Ir_3(\mu\text{-CO})(\mu\text{-S-t-Bu})_3(CO)_4(PMe_3)_2]$ crystallizes in space group $P2_1/c$ with $a = 16.521$ (3) Å, $b = 10.060$ (3) Å, $c = 21.295$ (4) Å, $\beta = 90.23$ (1)°, and $Z = 4$. On the basis of 1746 unique reflections, the structure was refined by full-matrix least-squares techniques to $R = 0.059$ and $R_w = 0.072$. The structure of the trinuclear entity ressembles that of $[Ir_2(\mu\text{-CO})(\mu\text{-S-}t\text{-Bu})(CO)_2(\text{S-}t\text{-Bu})(PMe_3)]$, owing to the Ir–Ir separation of 2.712 (3) Å and the presence of the bridging CO and S-*t*-Bu ligands. Infrared studies of these two complexes and of their CO loss in solution to form the disubstituted complex $[Ir_2(\mu\text{-S-}t\text{-Bu})_2(CO)_2(PMe_3)_2]$ allow us to propose a new pathway for this type of dinuclear iridium complexes to the CO substitution by tertiary phosphine ligands.

In previous publications we have described the synthesis and the structures of dinuclear bridged d^8 metal complexes $[Rh_2(\mu\text{-SR})_2(CO)_2L_2]$ and $[Ir_2(\mu\text{-SBu})_2(CO)_2L_2]$[4,5] (L = trialkylphosphine or phosphite) obtained by addition of 2 mol of ligand L to the parent compounds $[Rh_2(\mu\text{-SR})_2(CO)_4]$ and $[Ir_2(\mu\text{-S-}t\text{-Bu})_2(CO)_4]$, respectively. Focusing our attention to the substitution process, we proposed for the rhodium complexes as intermediate species $[Rh_2(\mu\text{-SR})_2(CO)_4L_2]$ with the two phosphorus ligands in the apical positions of two square pyramids sharing an edge. This structure was proposed from spectroscopic arguments.[2] Besides, examination of the IR and ^1H NMR spectra for the iridium complexes gave evidence for the labile species $[Ir_2(\mu\text{-S-}t\text{-Bu})_2(CO)_3L]$[4] in equilibrium with the non- and disubstituted complexes.

In order to gain more insight into the substitution process we found it an advantage to use the high solubility of the complex $[Ir_2(\mu\text{-S-}t\text{-Bu})_2(CO)_4]$ in any organic solvent and particularly in noncoordinating solvents such as pentane. The addition of 2 mol of ligand (in our case trimethylphosphine) was carried out in very concentrated solutions under a CO atmosphere, and a mixture

(1) Ecole Nationale Supérieure de Chimie, F-31077 Toulouse Cedex, France.

(2) Kalck, P.; Poilblanc, R. *Inorg. Chem.* **1975**, *14*, 2779-2784.

(3) Bonnet, J. J.; Kalck, P.; Poilblanc, R. *Inorg. Chem.* **1977**, *16*, 1514-1518.

(4) de Montauzon, D.; Kalck, P.; Poilblanc, R. *J. Organomet. Chem.* **1980**, *186*, 121-130.

(5) Bonnet, J. J.; Thorez, A.; Maisonnat, A.; Galy, J.; Poilblanc, R. *J. Am. Chem. Soc.* **1979**, *101*, 5940-5949.

(6) de Montauzon, D.; Poilblanc, R. "Inorganic Synthesis Series"; Wiley-Interscience: New York; pp 237-240.

0002-7863/82/1504-3069$01.25/0 © 1982 American Chemical Society

of two kinds of crystals was obtained, which, owing to their lability when dissolved, was analyzed by X-ray diffraction techniques. Characteristics of these two unexpected structures and examination of the loss of CO in solution led us to rationalize the formation of the novel compounds as part of a new pathway for the CO substitution by phosphine ligands in this type of dinuclear complex.

Experimental Section

All reactions were carried out under an atmosphere of dry, oxygen-free nitrogen, using Schlenk tubes and vacuum line procedures. The solvents were distilled, stored on molecular sieves, and saturated with nitrogen prior to use. Tricyclohexylphosphine (PCy_3) was of commercial origine.

Synthesis of the complexes $[Ir_2(\mu\text{-S-}t\text{-Bu})_2(CO)_4]$ (**1**), $[Ir_2(\mu\text{-S-}t\text{-Bu})(CO)_2(PMe_3)_2]$ (**2**), $[Ir_2(\mu\text{-S-}t\text{-Bu})_2(CO)_3(PMe_3)]$ (**3**), and $[Rh_2(\mu\text{-S-}t\text{-Bu})_2(CO)_4(PCy_3)_2]$ (**4**) was carried out according to the procedures described elsewhere.[2,4,6]

Infrared spectra were recorded with a Perkin-Elmer 225 grating spectrometer in hexadecane solutions or in cesium bromide pellets with a calibration for the carbonyl stretching region by water-vapor lines. Elemental analyses were performed by the Service Central de Microanalyse du C.N.R.S. ^1H NMR spectra were obtained on a Varian A-60 A spectrometer (benzene or dichloromethane solutions). Mass spectra were recorded on a Varian MAT 311 A spectrometer. Melting points were determined in air.

Isolation of the Compounds $[Ir_2(\mu\text{-CO})(\mu\text{-S-}t\text{-Bu})(CO)_2(S\text{-}t\text{-Bu})(PMe_3)_3]$ (5) and $[Ir_3(\mu\text{-CO})(\mu\text{-S-}t\text{-Bu})_3(CO)_4(PMe_3)_2]$ (6). A 0.675-g amount of **1** (1 mmol) was dissolved at room temperature in 6 mL of hexane, and in a small Schlenk tube (capacity 10–12 mL) 0.203 mL of trimethylphosphine was added with vigorous stirring. The yellow-brown solution became immediately orange. The stirring was maintained for 2 min. First, truncated octahedral red single crystals appeared. If the crystallization is performed overnight at room temperature, then a yellow complex cocrystallizes as small or flat parallelepipeds with the previous ones.

After 1 h at −20 °C the supernatant solution was removed and the products were washed twice with 10 mL of cold hexane and quickly dried in vacuo. All of the starting material was transformed.

The two compounds were air stable for several weeks at 20 °C. Any attempt to recrystallize the two complexes was unsuccessful; indeed complex **2** was in any case the final product.

Compounds **5** and **6** were handpicked under a microscope.

5 can be formulated as $[Ir_2(\mu\text{-CO})(\mu\text{-S-}t\text{-Bu})(CO)_2(S\text{-}t\text{-Bu})(PMe_3)_3]$, mp 124 °C, with gas evolution. Anal. Calcd for $C_{20}H_{45}Ir_2O_3P_3S_2$: C, 27.45; H, 5.18; S, 7.32. Found: C, 27.35; H, 5.11; S. 7.07. Calculated molecular weight, 875 deduced from the density measured in ZnI_2 aqueous solution and the volume of the unit cell, and 872 assuming 8 dinuclear molecules per unit cell.

6 can be formulated as $[Ir_3(\mu\text{-CO})(\mu\text{-S-}t\text{-Bu})_3(CO)_4(PMe_3)_2]$, mp 96 °C, with gas loss. Anal. Calcd for $C_{23}H_{45}Ir_3O_5P_2S_3$: C, 24.31; H, 3.99; S, 8.45. Found: C, 24.06; H, 4.01; S, 8.10. Calculated weight, 1136 deduced from the density measured in ZnI_2 aqueous solution and the volume of the unit cell, and 1135, assuming 4 dinuclear molecules per unit cell.

Collection and Reduction of the X-ray Data. A. Compound 5. Preliminary photographic data revealed that crystals of **5** belong to the tetragonal system and show systematic extinctions (hhl, $l = 2n + 1$ and $h00$, $h = 2n + 1$) consistent with the space group D^4_{2d}–$P\bar{4}2_1c$. All cell constants were obtained by a least-squares refinement of the setting angles of 25 automatically centered reflections that had been chosen from diverse regions of reciprocal space with $23 < 2\theta(Mo) < 27°$. These cell constants and other pertinent data are presented in Table I. Intensity data were collected at room temperature on a computer-controlled CAD 4-Nonius four-circle diffractometer. A total of 4775 intensities were recorded out to $2\theta(Mo) < 50°$. After processing the data,[7] using a value of p of 0.03, those 2313 unique reflections having $F_o^2 > 2\sigma(F_o^2)$ were used in subsequent calculations.

B. Compound 6. Preliminary film data showed that crystals of **6** belong to the monoclinic system and show systematic extinctions ($0k0$, $k = 2n + 1$; $h0l$, $l = 2n + 1$) consistent with the space group C^5_{2h}–$P2_1/c$.

Table I. Summary of Crystal Data and Intensity Collection

compd	$[(\mu\text{-CO})(\mu\text{-S-}t\text{-Bu})Ir_2(\text{S-}t\text{-Bu})(CO)_2(PMe_3)_3]$	$[(\mu\text{-CO})(\mu\text{-S-}t\text{-Bu})_3Ir_3(CO)_4(PMe_3)_2]$
formula	$C_{20}H_{45}Ir_2O_3P_3S_2$	$C_{23}H_{45}Ir_3O_5P_2S_3$
formula weight, amu	875.03	1136.35
a (at 22 °C), Å	15.334 (2)	16.521 (3)
b, Å	15.334	10.060 (3)
c, Å	26.623 (4)	21.295 (4)
β, deg		90.23 (1)
V, Å^3	6260	3539
Z	8	4
density (calcd), g cm^{-3}	1.857	2.132
density (measured in aqueous ZnI_2), g cm^{-3}	1.850	2.13
space group	D^4_{2d}–$P\bar{4}2_1c$	C^5_{2h}–$P2_1/c$
crystal dimensions, mm		0.420 × 0.286 × 0.071
crystal volume, mm^3		0.02031
boundary faces of the prism		{010}, {100}, {10$\bar{2}$}
radiation	Mo Kα from monochromator (λ(Mo Kα$_1$) = 0.7093 Å)	Mo Kα from monochromator
linear absorption coeff, cm^{-1}		53.94
transmission factors		0.166–0.507
take-off angle, deg	3.0	4.5
2θ limits, deg	2.5–50	2.5–44
final no. of variables	257	191
unique data used	$2313 F_o^2 > 2\sigma(F_o^2)$	$1746 F_o^2 > 3\sigma(F_o^2)$
$R = \Sigma\|\|F_o\| - \|F_c\|\|/\Sigma\|F_o\|$	0.045	0.059
$R_w = (\Sigma w(\|F_o\| - \|F_c\|)^2/\Sigma F_o^2)^{1/2}$	0.035	0.072
stand. error in an obs of unit wt, e	1.42	1.75

Cell constants were obtained by a least-squares refinement of the setting of 25 automatically centered reflections with $22 < 2\theta(Mo) < 26°$. These cell constants and other pertinent data are listed in Table I. Intensity data were collected at room temperature. A total of 4806 intensities were recorded out to $2\theta(Mo) < 46°$ from a crystal of very poor quality. After processing[7] the data, only those 1746 unique reflections having $F_o^2 > 3\sigma(F_o^2)$ were used in subsequent calculations.

Solution and Refinement of the Structures. Complex 5. The two iridium atoms together with the bridging sulfur atom were located in a normal Patterson synthesis. The positions of the remaining nonhydrogen atoms were obtained through the usual combination of full-matrix least-squares refinements and difference Fourier syntheses. Atomic scattering factors for the nonhydrogen atoms were taken from the usual tabulation.[8] Anomalous dispersion terms for the Ir, S, and P atoms were included in F_c.[9] Refinement of an isotropic model converged to values of R and R_w of 0.058 and 0.062. Futher full-matrix least-squares cycles of refinement were performed by using anisotropic thermal parameters for all atoms; the last one converged to values of R and R_w of 0.045 and 0.035. In the final difference Fourier map the highest peaks of density 0.6–0.85 eÅ^{-3} (12–17% of the density of a carbon atom found in previous difference Fourier maps) are featureless.

The final positional and thermal parameters of all nonhydrogen atoms are presented in Table II. The observed and calculated structure amplitudes for the data used appear in Table III.[10] The root-mean-square

(7) All calculations have been performed by using the CII IRIS 80 computer of the "Centre Interuniversitaire de Calcul de Toulouse". In addition to various local programs, modified versions of the following ones were employed: Ibers' AGNOST absorption program, which includes both the Coppens–Leiserrowitz–Rabinovich logic for Gaussian integration and the Tompa–de Meulenaur analytical method; Zalkin's FORDAP Fourier summation program; Johnson's ORTEP thermal ellipsoid plotting program; Busing and Levy's ORFFE error function program; Ibers's NUCLS full-matrix least-squares program, which in its nongroup form resembles the Busing and Levy's ORFLS program.

(8) Cromer, D. T.; Waber, J. T. "International Tables for X-ray Crystallography"; Kynoch Press: Birmingham, England, 1974; Vol. IV, Table 2.2.A.

(9) Ibers, J. A.; Hamilton, W. C. *Acta Crystallogr.* **1964**, *17*, 781–782.

(10) See paragraph at end of paper regarding supplementary material.

Table II. Positional and Thermal Parameters for the Atoms of $[(\mu\text{-CO})(\mu\text{-S-}t\text{-Bu})Ir_2(S\text{-}t\text{-Bu})(CO)_2(PMe_3)_3]$[a]

atoms	X	Y	Z	β_{11} or B (Å^2)	β_{22}	β_{33}	β_{12}	β_{13}	β_{23}
Ir(1)	0.23818 (4)	0.26322 (5)	0.11265 (2)	3.06 (4)	3.75 (4)	1.06 (1)	−0.09 (3)	0.02 (2)	0.24 (2)
Ir(2)	0.37937 (4)	0.28399 (5)	0.17217 (3)	3.00 (3)	4.56 (4)	0.95 (1)	−0.03 (3)	0.11 (2)	0.02 (2)
S(1)	0.3313 (3)	0.1477 (3)	0.1377 (2)	3.8 (2)	3.6 (2)	1.35 (7)	−0.1 (2)	0.1 (1)	0.3 (1)
S(2)	0.3051 (3)	0.2512 (3)	0.0268 (2)	4.9 (2)	4.9 (3)	1.15 (7)	−1.0 (2)	0.2 (1)	0.1 (1)
P(1)	0.1975 (3)	0.4016 (3)	0.0896 (2)	4.4 (3)	4.4 (3)	1.38 (8)	0.1 (2)	0.4 (1)	0.5 (1)
P(2)	0.5101 (3)	0.2709 (4)	0.1233 (2)	3.4 (2)	7.0 (3)	1.34 (8)	−0.5 (2)	0.2 (1)	−0.3 (1)
P(3)	0.4280 (3)	0.2666 (4)	0.2545 (2)	4.4 (3)	7.9 (4)	1.37 (8)	0.6 (3)	0.0 (1)	0.4 (2)
O(1)	0.2013 (8)	0.3176 (9)	0.2185 (5)	3.4 (7)	8.8 (9)	1.4 (2)	1.5 (6)	−0.6 (3)	−0.2 (4)
O(2)	0.0533 (9)	0.194 (1)	0.1027 (6)	3.8 (7)	7.8 (10)	3.5 (4)	−2.2 (7)	−0.6 (4)	0.7 (5)
O(3)	0.398 (1)	0.4808 (9)	0.1780 (7)	9 (1)	5.0 (8)	3.1 (4)	−2.5 (8)	−0.2 (6)	−1.4 (5)
C(1)	0.247 (1)	0.294 (1)	0.1837 (7)	3.3 (9)	3.9 (9)	1.6 (3)	−0.5 (8)	−0.2 (5)	0.5 (4)
C(2)	0.127 (1)	0.216 (1)	0.1057 (6)	7 (1)	4.0 (10)	1.0 (2)	−2.1 (10)	−0.6 (5)	0.4 (5)
C(3)	0.391 (1)	0.410 (2)	0.1741 (7)	1.8 (8)	14 (2)	0.7 (3)	−1 (1)	0.5 (5)	−0.9 (8)
C(4)	0.283 (1)	0.061 (1)	0.1788 (7)	6 (1)	4.9 (10)	1.5 (3)	0.8 (9)	−0.4 (6)	1.1 (5)
C(5)	0.237 (2)	0.097 (2)	0.2248 (9)	7.6 (6)					
C(6)	0.216 (2)	0.008 (2)	0.1494 (10)	9.2 (7)					
C(7)	0.359 (2)	0.004 (2)	0.195 (1)	9.4 (7)					
C(8)	0.254 (1)	0.165 (1)	−0.0111 (6)	4 (1)	3.7 (9)	1.6 (3)	−1.0 (8)	−0.2 (5)	−0.2 (4)
C(9)	0.418 (1)	0.256 (2)	0.5157 (8)	3.3 (10)	16 (2)	1.9 (4)	0 (1)	0.4 (5)	0.3 (9)
C(10)	0.304 (2)	0.336 (1)	0.4688 (9)	10 (2)	3 (1)	3.0 (5)	1 (1)	1.6 (8)	2.2 (6)
C(11)	0.345 (1)	0.184 (2)	0.4436 (7)	6 (1)	9 (1)	1.1 (3)	−1 (1)	1.3 (5)	−1.2 (6)
C(12)	0.281 (1)	0.471 (1)	0.0603 (7)	7 (1)	4 (1)	1.7 (3)	−0.5 (20)	1.0 (6)	0.2 (5)
C(13)	0.109 (1)	0.408 (1)	0.0452 (8)	3.0 (9)	7 (1)	2.6 (4)	0.1 (9)	−1.6 (6)	1.3 (6)
C(14)	0.156 (1)	0.471 (1)	0.1388 (8)	9 (1)	4 (1)	2.1 (4)	2.9 (20)	−0.4 (7)	−1.0 (6)
C(15)	0.021 (2)	0.145 (2)	0.4247 (8)	11 (2)	8 (2)	1.7 (4)	2 (1)	−0.9 (7)	1.3 (6)
C(16)	0.526 (1)	0.175 (2)	0.0857 (8)	6 (1)	8 (1)	1.8 (4)	0 (1)	1.9 (6)	−1.6 (6)
C(17)	0.616 (1)	0.282 (2)	0.1585 (8)	6 (1)	14 (2)	1.8 (4)	−3 (2)	−0.3 (6)	−0.4 (8)
C(18)	0.344 (1)	0.266 (2)	0.3030 (7)	8 (1)	15 (2)	1.0 (3)	2 (2)	1.7 (5)	0.5 (8)
C(19)	0.497 (2)	0.356 (2)	0.2743 (9)	10 (2)	9 (2)	2.4 (5)	−4 (1)	−2.7 (9)	−0.1 (8)
C(20)	0.494 (1)	0.173 (2)	0.2742 (8)	5 (1)	12 (2)	2.0 (4)	3 (1)	−0.6 (7)	2.0 (8)

[a] Estimated standard deviations in the least significant figure(s) are given in parentheses in this and all subsequent tables. The form of the anisotropic thermal ellipsoid is $\exp[-(\beta_{11}h^2 + \beta_{22}k^2 + \beta_{33}l^2 + 2\beta_{12}hk + 2\beta_{13}hl + 2\beta_{23}kl)]$. The quantities given in the table are the thermal coefficients $\times 10^5$.

Table V. Positional and Thermal Parameters for the Nongroup Atoms of $[(\mu\text{-CO})(\mu\text{-S-}t\text{-Bu})_3Ir_3(CO)_4(PMe_3)_2]$[a]

atom	X	Y	Z	β_{11} or B (Å^2)	β_{22}	β_{33}	β_{12}	β_{13}	β_{23}
Ir(1)	0.2084 (1)	−0.1305 (2)	−0.17443 (9)	2.73 (8)	8.7 (3)	1.67 (5)	0.0 (1)	0.74 (5)	0.09 (10)
Ir(2)	0.1661 (1)	−0.1920 (2)	−0.05497 (9)	3.08 (9)	9.1 (3)	1.79 (5)	0.3 (1)	0.87 (5)	0.3 (1)
Ir(3)	0.4185 (1)	−0.2275 (2)	−0.0712 (1)	2.96 (9)	11.9 (3)	2.96 (6)	0.2 (1)	0.05 (6)	0.0 (1)
S(1)	0.1636 (7)	−0.343 (1)	−0.1414 (6)	3.7 (6)	7 (2)	2.3 (3)	0.3 (8)	0.8 (3)	−0.1 (6)
S(2)	0.3508 (8)	−0.221 (2)	−0.1680 (7)	3.5 (6)	31 (4)	3.2 (5)	5 (1)	0.1 (4)	−3 (1)
S(3)	0.2975 (9)	−0.290 (2)	−0.0166 (9)	3.7 (7)	19 (3)	6.5 (7)	−1 (1)	−0.1 (6)	6 (1)
P(1)	0.2609 (8)	0.081 (1)	−0.1860 (6)	4.5 (7)	9 (2)	2.5 (4)	−0.2 (9)	1.1 (4)	0.2 (7)
P(2)	0.1864 (9)	−0.027 (2)	0.0185 (6)	4.7 (7)	12 (2)	2.1 (4)	−0.1 (10)	0.6 (4)	−1.4 (7)
O(1)	0.061 (2)	0.010 (3)	−0.123 (1)	4.6 (8)					
O(2)	0.147 (2)	−0.128 (4)	−0.303 (2)	5.7 (8)					
O(3)	0.026 (3)	−0.311 (4)	0.022 (2)	8 (1)					
C(1)	0.116 (3)	−0.054 (5)	−0.116 (2)	3 (1)					
C(2)	0.172 (2)	−0.131 (5)	−0.245 (2)	3.1 (9)					
C(3)	0.082 (4)	−0.280 (6)	−0.005 (3)	5 (2)					
C(6)	0.118 (4)	0.110 (8)	0.017 (3)	10 (2)					
C(7)	0.173 (4)	−0.083 (7)	0.103 (3)	8 (2)					
C(8)	0.286 (4)	0.050 (8)	0.024 (3)	9 (2)					
C(9)	0.287 (4)	0.119 (7)	−0.271 (3)	8 (2)					
C(10)	0.187 (4)	0.220 (8)	−0.175 (3)	10 (2)					
C(11)	0.353 (4)	0.122 (7)	−0.139 (3)	8 (2)					
C(12)	0.061 (3)	−0.385 (6)	−0.170 (3)	6 (1)					
C(13)	−0.002 (3)	−0.276 (6)	−0.172 (2)	5 (1)					
C(14)	0.072 (4)	−0.447 (7)	−0.235 (3)	7 (2)					
C(15)	0.034 (3)	−0.506 (6)	−0.126 (2)	5 (1)					

atom	X	Y	Z	B, Å^2
C(16)	0.301 (4)	−0.456 (6)	0.014 (3)	6 (1)
C(17)	0.218 (5)	−0.510 (8)	0.035 (4)	10 (2)
C(18)	0.363 (6)	−0.477 (10)	0.062 (4)	13 (3)
C(19)	0.318 (6)	−0.55 (1)	−0.043 (5)	14 (3)
C(20)	0.388 (3)	−0.335 (6)	−0.229 (2)	5 (1)
C(21)	0.333 (8)	−0.31 (1)	−0.291 (6)	7 (3)
C(22)	0.476 (9)	−0.31 (2)	−0.242 (7)	8 (4)
C(23)	0.366 (6)	−0.47 (1)	−0.198 (5)	5 (3)
C′(21)	0.465 (6)	−0.40 (1)	−0.209 (5)	5 (3)
C′(22)	0.327 (6)	−0.42 (1)	−0.261 (5)	5 (2)
C′(23)	0.424 (8)	−0.24 (1)	−0.280 (6)	9 (4)

[a] Estimated standard deviations in the least significant figure(s) are given in parentheses in this and all subsequent tables. The form of the anisotropic thermal ellipsoid is $\exp[-(\beta_{11}h^2 + \beta_{22}k^2 + \beta_{33}l^2 + 2\beta_{12}hk + 2\beta_{13}hl + 2\beta_{23}kl)]$. The quantities β_{ij}'s given in the table are the thermal coefficients $\times 10^5$.

amplitudes of thermal displacement along principal axes appear in Table IV.[10]

Complex 6. From a normal Patterson synthesis, the three iridium and three sulfur atoms were found. Through the usual combination of full-matrix least-squares refinements and difference Fourier syntheses the remaining nonhydrogen atoms were located. However, several problems arised during the refinement of an isotropic model: (i) large thermal motions about the *t*-Bu group carbon atoms attached to S(3) were observed but no disorder was detected; (ii) a difference Fourier map calculated in oblic planes perpendicular to the S(2)–C(20) direction revealed the presence of six separate peaks of about the same magnitude, showing clearly alternative positions for the three carbon atoms attached to C(20) (it was decided to affect an occupancy factor of 0.5 for each for these six carbon atoms, the remaining atoms being refined with an occupancy factor of 1), (iii) due to the very poor quality of the data set only the Ir, S, and P atoms were refined by using anisotropic thermal prameters; and (iv) because of abnormal Ir–C bond distances about Ir(3), the four carbon and O atoms of the carbonyl groups attached to Ir(3) were treated as rigid groups with imposed C–O distances of 1.15 Å and an imposed CO–CO vector angle of 90°. Atomic scattering factors and anomalous

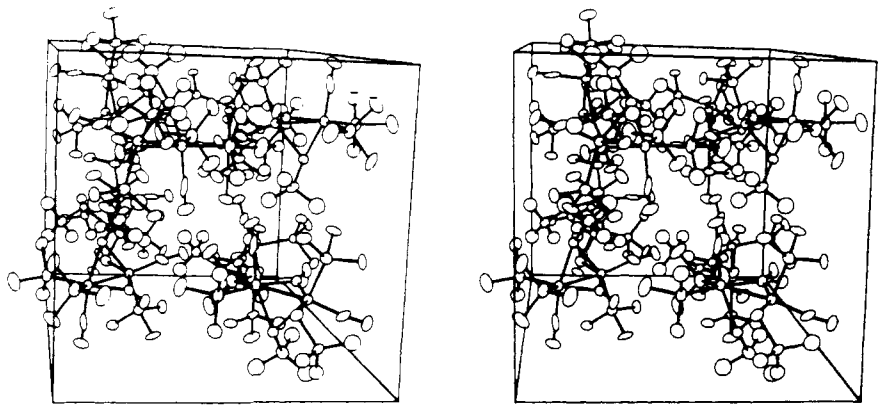

Figure 1. Stereoscopic view of a unit cell of $[Ir_2(\mu\text{-}CO)(\mu\text{-}S\text{-}t\text{-}Bu)(CO)_2(S\text{-}t\text{-}Bu)(PMe_3)_3]$. The x axis is horizontal from left to right, the y axis is perpendicular from bottom to top, and the z axis comes out of the paper. The vibrational ellipsoids are drawn at the 30% level. Hydrogen atoms are omitted.

Table VI. Derived Parameters for the Rigid Group Atoms of $[(\mu\text{-}CO)(\mu\text{-}S\text{-}t\text{-}Bu)_3Ir_3(CO)_4(PMe_3)_2]$[a]

atoms	x	y	z	B, Å^2	atoms	x	y	z	B, Å^2
C(4)	0.515 (2)	−0.153 (5)	−0.111 (1)	9 (2)	O(4)	0.576 (3)	−0.119 (5)	−0.131 (1)	10 (1)
C(5)	0.466 (2)	−0.211 (5)	−0.003 (2)	6 (1)	O(5)	0.496 (3)	−0.213 (5)	0.046 (1)	11 (1)

	rigid group parameters					
group	x_C	y_C	z_C	δ	ϵ	η
CO	0.491 (2)	−0.182 (4)	−0.057 (2)	−0.95 (4)	1.98 (2)	1.19 (9)

[a] x_C, y_C, and z_C are the fractional coordinates of the origin of the rigid group. The rigid group orientation angles δ, ϵ, and η (radians) have been defined previously: S. J. La Placa and J. A. Ibers. *Acta Crystallogr.*, 18, 511 (1965).

Table IX. Selected Distances (Å) in $[(\mu\text{-}CO)(\mu\text{-}S\text{-}t\text{-}Bu)Ir_2(S\text{-}t\text{-}Bu)(CO)_2(PMe_3)]$

Ir(1)–Ir(2)	2.702 (1)	P(1)–C(12)	1.84 (2)
Ir(1)–S(1)	2.371 (4)	P(1)–C(13)	1.81 (2)
Ir(2)–S(1)	2.400 (4)	P(1)–C(14)	1.80 (2)
Ir(1)–S(2)	2.512 (4)	P(2)–C(15)	1.82 (2)
Ir(1)–C(1)	1.95 (2)	P(2)–C(16)	1.80 (2)
Ir(2)–C(1)	2.07 (2)	P(2)–C(17)	1.88 (2)
Ir(1)–P(1)	2.295 (5)	P(3)–C(18)	1.83 (2)
Ir(1)–C(2)	1.86 (2)	P(3)–C(19)	1.81 (2)
Ir(2)–P(2)	2.398 (5)	P(3)–C(10)	1.83 (2)
Ir(2)–P(3)	2.332 (5)	C(4)–C(5)	1.52 (3)
Ir(2)–C(3)	1.93 (3)	C(4)–C(6)	1.51 (3)
C(1)–O(1)	1.21 (2)	C(4)–C(7)	1.52 (3)
C(2)–O(2)	1.19 (2)	C(8)–C(9)	1.47 (2)
C(3)–O(3)	1.10 (3)	C(8)–C(10)	1.56 (3)
S(1)–C(4)	1.88 (2)	C(8)–C(11)	1.55 (2)
S(2)–C(8)	1.84 (2)		

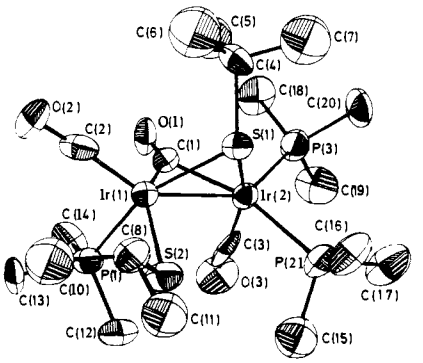

Figure 2. A perpective representation of a molecule of $[Ir_2(\mu\text{-}CO)(\mu\text{-}S\text{-}t\text{-}Bu)(CO)_2(S\text{-}t\text{-}Bu)(PMe_3)_3]$. The vibrational ellipsoids are drawn at 50% probability level. The C(9) carbon atom attached to the C(8) of the terminal S-t-Bu group has been omitted for clarity.

dispersion terms for the Ir, S, and P atoms were from the usual source.[8] The last full-matrix least-squares cycle converged to values of R and R_w of 0.059 and 0.072. The final positional and thermal parameters (B's or β_{ij}'s) of all nonhydrogen atoms are listed in Table V. The observed and calculated structure amplitudes for the data used appear in Table VII.[10]

Table X. Selected Angles (Deg) in $[(\mu\text{-}CO)(\mu\text{-}S\text{-}t\text{-}Bu)Ir_2(S\text{-}t\text{-}Bu)(CO)_2(PMe_3)_3]$

S(1)–Ir(1)–C(1)	82.6 (5)	Ir(1)–S(1)–Ir(2)	69.0 (1)	C(16)–P(2)–C(17)	103.4 (1.1)
S(1)–Ir(1)–S(2)	87.4 (2)	Ir(1)–S(1)–C(4)	117.0 (6)	Ir(2)–P(3)–C(18)	116.0 (7)
S(1)–Ir(1)–C(2)	106.6 (6)	Ir(2)–S(1)–C(4)	121.1 (6)	Ir(2)–P(3)–C(19)	111.9 (8)
P(1)–Ir(1)–S(1)	158.3 (2)	Ir(1)–C(1)–Ir(2)	84.4 (7)	Ir(2)–P(3)–C(20)	122.4 (8)
P(1)–Ir(1)–S(2)	86.3 (2)	Ir(1)–C(1)–O(1)	140.8 (1.3)	C(18)–P(3)–C(19)	102.3 (1.3)
S(2)–Ir(1)–C(1)	150.6 (5)	Ir(2)–C(1)–O(1)	134.4 (1.2)	C(18)–P(3)–C(20)	100.8 (1.1)
S(2)–Ir(1)–C(2)	104.7 (5)	Ir(1)–C(2)–O(2)	173.0 (1.8)	C(19)–P(3)–C(20)	100.6 (1.2)
P(1)–Ir(1)–C(2)	95.0 (6)	Ir(2)–C(3)–O(3)	176.0 (2.1)	S(1)–C(4)–C(5)	112.9 (1.4)
P(1)–Ir(1)–C(1)	92.9 (5)	Ir(1)–S(2)–C(8)	112.3 (6)	S(1)–C(4)–C(6)	110.0 (1.4)
C(2)–Ir(1)–C(1)	104.6 (7)	Ir(1)–P(1)–C(12)	117.0 (7)	S(1)–C(4)–C(7)	105.0 (1.6)
S(1)–Ir(2)–C(1)	79.6 (5)	Ir(1)–P(1)–C(13)	115.5 (7)	C(5)–C(4)–C(6)	107.6 (1.9)
S(1)–Ir(2)–P(2)	88.6 (2)	Ir(1)–P(1)–C(14)	116.5 (7)	C(5)–C(4)–C(7)	110.3 (1.8)
S(1)–Ir(2)–P(3)	111.0 (2)	C(12)–P(1)–C(13)	102.5 (9)	C(6)–C(4)–C(7)	111.2 (1.9)
S(1)–Ir(2)–C(3)	154.8 (6)	C(12)–P(1)–C(14)	102.5 (9)	S(2)–C(8)–C(9)	113.7 (1.3)
P(2)–Ir(2)–P(3)	103.5 (2)	C(13)–P(1)–C(14)	100.3 (9)	S(2)–C(8)–C(10)	110.6 (1.3)
P(2)–Ir(2)–C(9)	91.3 (5)	Ir(2)–P(2)–C(15)	113.4 (9)	S(2)–C(8)–C(11)	103.6 (1.2)
P(2)–Ir(2)–C(1)	155.6 (5)	Ir(2)–P(2)–C(16)	118.9 (7)	C(9)–C(8)–C(10)	109.6 (1.9)
P(3)–Ir(2)–C(3)	93.5 (6)	Ir(2)–P(2)–C(17)	116.3 (7)	C(9)–C(8)–C(11)	111.0 (1.6)
P(3)–Ir(2)–C(1)	100.7 (5)	C(15)–P(2)–C(16)	100.3 (1.0)	C(10)–C(8)–C(11)	108.1 (1.6)
C(3)–Ir(2)–C(1)	90.5 (7)	C(15)–P(2)–C(17)	102.0 (1.2)		

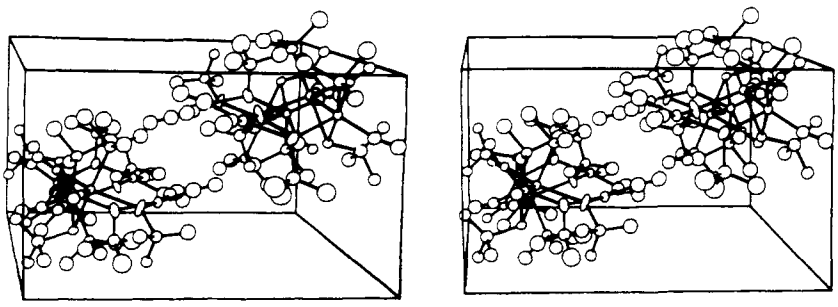

Figure 3. Stereoscopic view of a unit cell of $[Ir_3(\mu\text{-}CO)(\mu\text{-}S\text{-}t\text{-}Bu)_3(CO)_4(PMe_3)_2]$. The x axis is horizontal from left to right, the y axis is perpendicular from bottom to top, and the z axis comes out of the paper. The vibrational ellipsoids are drawn at the 25% level.

Table XI. Least-Squares Planes Calculations

(i) In 5[a]

(A) Atoms Defining Plane: S(1), S(2), P(1), C(1)

Equation of Plane: $13.118X + 7.630Y + 3.815Z - 6.011 = 0$

S(1)	-0.013 (4)	C(1)	0.168 (16)
S(2)	0.010 (4)	Ir(1)	-0.45
P(1)	-0.014 (5)		

(B) Atoms Defining Plane: S(1), C(1), P(2), C(3)

Equation of Plane: $5039X - 4.510Y + 23.894Z - 4.294 = 0$

S(1)	-0.000 (4)	C(3)	-0.013 (4)
C(1)	0.010 (4)	Ir(2)	-0.45
P(2)	0.001 (5)		

(ii) In 6[b]

Atoms Defining Plane: Ir(1), Ir(2), S(2), S(3)

Equation of Plane: $5.180X + 9.044Y + 6.4832Z + 1.232 = 0$

Ir(1)	0.001 (2)	S(1)	-1.939 (2)
Ir(2)	0.000 (2)	Ir(3)	0.882 (2)
S(2)	-0.041 (2)	C(1)	0.590 (2)
S(3)	0.041 (2)		

[a] X, Y, and Z are the fractional coordinates as in Table II. [b] X, Y, and Z are the fractional coordinates as in Table V.

For the Ir, S, and P atoms the root-mean-square components of thermal displacement along principal axes are presented in Table VIII.[10]

Results

Description of the Structures. The crystal structure of **5** consists of eight dinuclear molecules per unit cell. A stereoscopic packing diagram of the unit cell is shown in Figure 1. Selected bond distances and bond angles are given in Tables IX and X. Figure 2 shows a perspective view of molecule **5** along with the labeling scheme used elsewhere.

The overall coordination geometry closely resembles two square-pyramidal coordinated iridium atoms sharing an edge so that the two iridium atoms are bridged by a thiolato group and a CO ligand. The Ir(1) atom is bound to four atoms roughly in a plane (see Table X), i.e., S(1) and C(1) of the bridging groups and S(2) and P(1) of the terminal thiolato and trimethylphosphine ligands, respectively; the fifth position of the square pyramid is occupied by C(2) of the terminal carbonyl group. Ir(2) is also bound to four atoms roughly in a plane (see Table X), namely S(1) and C(1) of the previous bridging groups and P(2) and C(3) of trimethylphosphine and terminal carbonyl ligands, respectively; P(3) of a terminal trimethylphosphine ligand occupies the fifth position. Ir(1) and Ir(2) are 0.045 Å out of the planes and the "flap" angle, i.e., the dihedral angle between the two planes around the iridium atoms, is 71.6° (Table X). The separation of the two iridium atoms is 2.702 (1) Å, suggesting a metal–metal bond in agreement with the observed diamagnetism and the E.A.N. rule. This distance is very comparable to those found in $[Ir_2(NO)_4(PPh_3)_2]$ (2.717 Å),[11] $[Ir_2(C_5H_5)_2(CO)_2(C_6H_4)]$ (2.7166 Å),[12] $[Ir_2(C_5Me_5)(CO)_2(CF_3C_2CF_3)_3H]$ (2.737 Å),[13] $[Ir_2(CO)_2(PPh_3)_2(C_{10}H_4S)_4Br_2]$ (2.676 Å),[14] $[Ir_2(\mu\text{-}S\text{-}t\text{-}Bu)_2(CO)_2(P(OMe)_3)_2H_2]$ (2.673 Å),[5] $[Ir_2(\mu\text{-}S)(\mu\text{-}CO)(CO)_2(PPh_2CH_2PPh_2)_2]$ (2.843 Å),[15] and $[Ir_2(\mu\text{-}S\text{-}t\text{-}Bu)_2(CO)_2(PMe_2Ph)_2I_2]$ (2.703 Å).[16]

P(1) and C(3) bound to Ir(1) and Ir(2), respectively, are trans to S(1) of the thiolato bridging ligand while P(2) and S(2) are trans to C(1) of the bridging carbonyl group. Thus P(1) and P(2) are mutually in trans positions with respect to the Ir(1)–Ir(2) bond. An Ir(1)–P(1) bond distance of 2.295 (5) Å compares well with the average Ir–P bonds of 2.31 Å found in $[Ir_2(\mu\text{-}S\text{-}t\text{-}Bu)_2(CO)_2(PMe_2Ph)_2I_2]$,[16] a dinuclear Ir(II) complex were the phosphorus atoms are trans to a sulfur atom of a thiolato bridging group, which is an analogous situation for P(1) in **5**. An Ir(2)–P(2) bond distance of 2.398 (5) Å is 0.103 Å (20σ) longer than Ir(1)–P(1), a huge lengthening that might be due to the trans influence of the carbonyl bridging group. Moreover this distance compares well with various values found in some mononuclear complexes of iridium, i.e., 2.403 (4) and 2.372 (4) Å in $[(IrCl(N_2Ph)(PMePh_2)_3)(PF_6)]$[17] or 2.389 (5), 2.398 (5), and 2.327 (5) Å in $[(IrO_2(PMe_2Ph)_4)(BPh_4)]$,[18] for example, but is the longest never observed to the best of our knowledge in dinuclear iridium species.

The slight difference observed for the Ir(1)–C(1) and Ir(2)–C(2) bond distances (1.95 (2) and 2.07 (2) Å, respectively) is not to be related to a "semibridging" carbonyl ligand. Although the angles around C(1), namely Ir(1)–C(1)–O(1) and Ir(2)–C(1)–O(1), are respectively 140.8 and 134.4°, the observed difference is rather due to the different environments of Ir(1) and Ir(2). Thus the carbonyl ligand C(1)–O(1) bridges the two iridium atoms rather symmetrically as in the "A-frame" complexes $[Ir_2(\mu\text{-}S)(\mu\text{-}CO)(CO)_2(Ph_2PCH_2PPh_2)_2]$,[15] $[(Rh_2(CO)_2(\mu\text{-}CO)(\mu\text{-}Cl)(Ph_2PCH_2PPh_2)_2)(BPh_4)]$,[19] and $[Pd_2Cl_2(\mu\text{-}CO)(Ph_2AsCH_2AsPh_2)_2]$,[20] and its platinum analogue[21] or $[Rh_2Br_2(\mu\text{-}CO)(Ph_2PCH_2PPh_2)_2]$[22] and $[Rh_2Cl_2(\mu\text{-}CO)(\mu\text{-}C_6H_6O_4)(Ph_2PCH_2PPh_2)_2]$;[23] the iridium –C(1) bond distances compare well with the value of 2.07 (1) Å found in the $[Ir_2(\mu\text{-}S)(\mu\text{-}CO)(CO)_2(Ph_2PCH_2PPh_2)_2]$ dinuclear complex. The C(1)–O(1) bond distance of 1.21 (2) Å agrees with those reported in the literature for other dinuclear complexes of rhodium and iridium exhibiting a bridging carbonyl ligand.[15,19,22]

(11) Angoletta, M.; Ciani, G.; Manassero, M.; Sansoni, M. *J. Chem. Soc., Chem. Commun.* **1973**, 789–789.
(12) Rausch, M. D.; Gastinger R. G.; Gardner S. A.; Brown, R. K.; Wood, J. S. *J. Am. Chem. Soc.* **1977**, *99*, 7870–7876.
(13) Corrigan, P. A.; Dickson, R. S.; Fallon, G. D.; Michel, L. J.; Mok, C. *Aust. J. Chem.* **1978**, *31*, 1937–1951.
(14) Teo, B. K.; Snyder-Robinson, P. A. *J. Chem. Soc., Chem. Commun.* **1979**, 255–256.
(15) Kubiak, C. P.; Woodcock, C.; Eisenberg, R. *Inorg. Chem.* **1980**, *19*, 2733–2739.
(16) Bonnet, J. J.; Kalck, P.; Poilblanc, R. *Angew. Chem., Int. Ed. Engl.* **1980**, *19*, 551–552.
(17) Cowie, M.; Haymore, B. L.; Ibers, J. A. *J. Am. Chem. Soc.* **1976**, *98*, 7608–7617.
(18) Nolte, M.; Singleton, E. *Acta Crystallogr., Sect. B* **1976**, *B32*, 1838–1841.
(19) Cowie, M. *Inorg. Chem.* **1979**, *18*, 286–292.
(20) Colton, R.; Mc Cormick, M. J.; Pannan, C. D. *Aust. J. Chem.* **1978**, *31*, 1425–1438.
(21) Brown, M. P.; Keith, A. N.; Manojlovic-Muir, L. J.; Muir, K. W.; Puddephatt, R. J.; Seddon, K. R. *Inorg. Chim. Acta* **1979**, *34*, L223–L224.
(22) Cowie, M.; Dwight, S. K. *Inorg. Chem.* **1980**, 2508–2513.
(23) Cowie, M.; Southern, T. G. *J. Organomet. Chem.* **1980**, *193*, C46–C50.

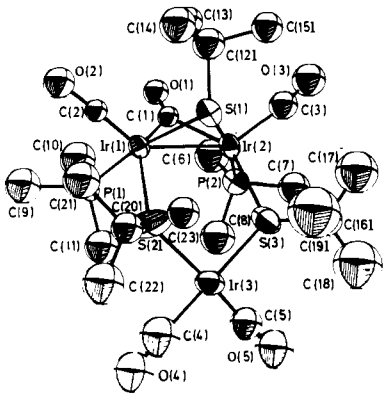

Figure 4. A perspective representation of a molecule of $[Ir_3(\mu\text{-Co})(\mu\text{-S-}t\text{-Bu})_3(CO)_4(PMe_3)_2]$. The vibrational ellipsoids are drawn at 50% probability level.

Table XII. Selected Distances (Å) in $[(\mu\text{-CO})(\mu\text{-S-}t\text{-Bu})_3Ir_3(CO)_4(PMe_3)_2]$

Ir(1)-Ir(2)	2.712 (3)	P(1)-C(10)	1.87 (7)
Ir(1)-Ir(3)	4.216 (3)	P(1)-C(11)	1.86 (6)
Ir(2)-Ir(3)	4.201 (3)	P(2)-C(6)	1.79 (7)
Ir(1)-C(1)	2.12 (4)	P(2)-C(7)	1.82 (7)
Ir(1)-S(1)	2.37 (1)	P(2)-C(8)	1.89 (6)
Ir(1)-S(2)	2.53 (1)	C(12)-C(13)	1.50 (7)
Ir(1)-P(1)	2.31 (1)	C(12)-C(14)	1.54 (7)
Ir(2)-C(1)	2.07 (5)	C(12)-C(15)	1.59 (7)
Ir(2)-S(1)	2.39 (1)	C(16)-C(17)	1.46 (9)
Ir(2)-S(3)	2.52 (1)	C(16)-C(18)	1.55 (9)
Ir(2)-P(2)	2.30 (1)	C(16)-C(19)	1.55 (9)
Ir(3)-S(2)	2.34 (2)	C(20)-C(21)	1.61 (11)
Ir(3)-S(3)	2.40 (2)	C(20)-C(22)	1.50 (11)
S(1)-C(12)	1.85 (6)	C(20)-C(23)	1.56 (11)
S(2)-C(20)	1.85 (5)	C(20)-C(21')[a]	1.50 (11)
S(3)-C(16)	1.78 (6)	C(20)-C(22')	1.47 (11)
P(1)-C(9)	1.91 (7)	C(20)-C(23')	1.54 (11)

[a] The primed atoms are those in alternative positions with the corresponding nonprimed atoms (see text).

Complex **5** is to our knowledge the first structurally characterized dinuclear complex of the group 8 metals in which a carbonyl ligand occupies the bridging site in preference to a thiolato group. This unexpected situation has to be compared to that found for instance in $[Rh_2Br_2(\mu\text{-CO})(Ph_2PCH_2PPh_2)_2]$,[22] where the carbonyl ligand is in the bridging position rather than the halide ligands.

No unusual intra- or intermolecular nonbonded contacts are observed in the structure.

The crystal structure of $[Ir_3(\mu\text{-S-}t\text{-Bu})_3(\mu\text{-CO})(CO)_4(PMe_3)_2]$ (**6**) consists of the packing of four trinuclear molecules. A stereoscopic packing diagram of the unit cell is shown in Figure 3. Selected bond distances and bond angles are given in Tables XII and XIII. Figure 4 shows a perspective view of molecule **6** that includes the labeling scheme used in this paper. The structure of a trinuclear unit could be described as a six-membered ring of either alternate Ir and S atoms in a "chair" conformation or C(1) instead of S(1) in a "boat" conformation type (see Table XI). It is thus the second example of a crown-like trinuclear complex.[24]

However, we prefer to point out that structure **6** resembles the structure of **5** if one substitutes the S(2)-Ir(3)-S(3) bridge with the terminal thiolato ligand attached to Ir(1) and a phosphine ligand bound to Ir(2) in **5**. Thus, as in **5**, the coordination geometry about Ir(1) and Ir(2) consists of two square-pyramidal coordinated iridium atoms sharing an edge in a way that these two metal atoms are bridged by a thiolato group and a CO ligand. The similarity between the two structures **5** and **6** can be reinforced by the following two features: the Ir(1)-Ir(2) bond distance of

Scheme I

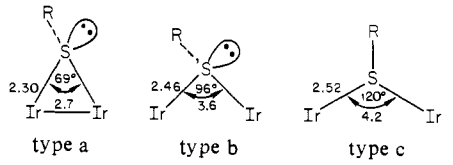

2.712 (3) Å in **6** is close to that of 2.702 (1) Å in **5** and the "flap" angle is 66.8° in **6** instead of 71.6° in **5**. These similarities are discussed further latter as an evidence for a new pathway for the substitution process in dinuclear iridium complexes. The main difference between **5** and **6** about the Ir(1) and Ir(2) coordination geometry arises from the mutual positions of the terminal carbonyl ligand and the trimethylphosphine ligands attached to Ir(2). Indeed the carbonyl group is in the axial position in **6** instead of the equatorial one in **5**, so that the overall modification about Ir(2) from **5** to **6** can be seen as the replacements of P(2) in **5** by S(3), of C(3) by P(2), and of P(3) by C(3). The various Ir-P bond distances observed are quite normal. The geometry of Ir(3) is of the square-planar type, as is usually found for an Ir(I) atom. An important feature in the present structure arises from the bond angles around the sulfur atoms. Indeed those around S(1) clearly show a tetrahedral environment, as is usually observed in thiolato-bridged dinuclear complexes.[3,5] However, those around S(2) and S(3) (cf. Table XII) are quite surprisingly consistent with a planar environment not yet reported in the literature to our knowledge. Such a feature could be a key to the variation of the geometry around S atoms observed in the thiolato-bridged complexes. Scheme I summarizes the situations observed in complexes of type a such as $[Ir_2(\mu\text{-S-}t\text{-Bu})_2(CO)_2(P(OMe)_3)_2H_2]$[6] and $[Ir_2(\mu\text{-S-}t\text{-Bu})_2(CO)_2(PMe_2Ph)_2I_2]$,[16] of type b such as $[Ir_2(\mu\text{-S-}t\text{-Bu})_2(CO)_2(P(OMe)_3)_2]$,[5] or of type c such as the present complex **6**. It shows the strong correlation between the Ir-S-Ir angle and the Ir-Ir and Ir-S distances so that the planarity around the sulfur atom requires a rather long iridium-iridium distance. Could the geometry of type c be taken into account for an endo-exo isomerization via a sulfur inversion in thiolato-bridged dimers with a planar intermediate?[25]

Infrared Study of the Complexes. Addition of 2 mol of the trimethylphosphine ligand to carbonyl complex **1**, $[Ir_2(\mu\text{-S-}t\text{-Bu})_2(CO)_4]$, in ~0.1-0.13 M solutions of pentane or hexane gave after crystallization the two complexes **5** and **6**. By handpicking the mixture of crystals, complexes **5** and **6** were found in a ratio of almost 3:2. IR analysis in the solid state on various samples failed to reveal the presence of any other compound than **5** and **6**. We did not find complex **2**; indeed its low solubility, which in hexane would have been a sufficient driving force for its crystallization or precipitation, leads us to admit that there is no tendency for it to form. This result seems to us very important for the mechanism of the substitution, since the addition of ligand was performed in a noncoordinating solvent.

Infrared spectra of complex **5** in CsBr pellets exhibit two terminal CO stretching bands at 1951 and 1941 cm^{-1} and one band at 1703 cm^{-1} that are characteristic of a bridging CO ligand. The first two ν_{CO} bands are reminiscent of those of complex **2**, the slight differences arising from the facts that in complex **5** the dihedral angle is constrained (~70° instead of ~124°),[5] the two CO ligands are mutually trans (cis for complex **2**), and the core is somewhat different. The 1705-cm^{-1} frequency is quite low and will be discussed later (vide infra). Infrared spectra of the same complex **5** in freshly prepared solutions of hexadecane did not

(24) Devillers, J.; Bonnet, J. J.; de Montauzon, D.; Galy, J.; Poilblanc, R. *Inorg. Chem.* **1980**, *19*, 154-159.

(25) This hypothesis has been rejected by Knox and co-workers,[26] who have considered that the ring inversion allows the endo-exo isomerization. We can notice that the syn-anti isomerism does require the inversion about a sulfur atom: this type of isomerization in some μ-thiolato platinum complexes was previously interpreted in terms of a process involving the inversion at the bridging sulfur atoms.[27]

(26) Hill, R.; Kelly, B. A.; Kennedy, F. G.; Knox, S. A. R.; Woodward, P. *J. Chem. Soc., Chem. Commun.* **1977**, 434-436.

(27) Brown, M. P.; Puddephatt, R. J.; Upton, C. E. E. *J. Chem. Soc., Dalton Trans.* **1976**, 2490-2494.

Table XIII. Selected Angles (Deg) in $[(\mu\text{-CO})(\mu\text{-S-}t\text{-Bu})_3Ir_3(CO)_4(PMe_3)_2]$

C(1)-Ir(1)-C(2)	106.3 (19)	P(2)-Ir(2)-S(3)	86.5 (6)	Ir(1)-P(1)-C(9)	112 (2)
C(1)-Ir(1)-S(1)	85.7 (13)	Ir(1)-S(1)-Ir(2)	69.5 (3)	Ir(1)-P(1)-C(10)	115 (2)
C(1)-Ir(1)-P(1)	90.1 (13)	Ir(1)-S(1)-C(12)	113.4 (19)	Ir(1)-P(1)-C(11)	117 (2)
C(1)-Ir(1)-S(2)	140.5 (13)	Ir(2)-S(1)-C(12)	114.1 (18)	C(9)-P(1)-C(10)	97 (3)
C(2)-Ir(1)-S(1)	99.0 (17)	Ir(1)-C(1)-Ir(2)	80.8 (17)	C(9)-P(1)-C(11)	106 (3)
C(2)-Ir(1)-P(1)	92.5 (17)	Ir(1)-C(1)-O(1)	135.2 (36)	C(10)-P(1)-C(11)	107 (3)
C(2)-Ir(1)-S(2)	113.2 (15)	Ir(2)-C(1)-O(1)	142.4 (37)	Ir(2)-P(2)-C(6)	116 (2)
S(1)-Ir(1)-P(1)	168.5 (5)	Ir(1)-S(2)-Ir(3)	119.9 (6)	Ir(2)-P(2)-C(7)	114 (2)
S(1)-Ir(1)-S(2)	87.1 (6)	Ir(1)-S(2)-C(20)	119.9 (17)	Ir(2)-P(2)-C(8)	119 (2)
P(1)-Ir(1)-S(2)	89.4 (6)	Ir(3)-S(2)-C(20)	116.6 (18)	C(6)-P(2)-C(7)	100 (3)
C(1)-Ir(2)-C(3)	110.9 (22)	Ir(2)-S(3)-Ir(3)	117.2 (6)	C(6)-P(2)-C(8)	104 (3)
C(1)-Ir(2)-S(1)	86.4 (13)	Ir(2)-S(3)-C(16)	120.8 (20)	C(7)-P(2)-C(8)	100 (3)
C(1)-Ir(2)-P(2)	90.0 (13)	Ir(3)-S(3)-C(16)	113.1 (20)	S(1)-C(12)-C(13)	118 (4)
C(1)-Ir(2)-S(3)	144.0 (13)	S(2)-Ir(3)-S(3)	92.2 (6)	S(1)-C(12)-C(14)	106 (4)
C(3)-Ir(2)-S(1)	96.7 (18)	S(2)-Ir(3)-C(4)	90.0[a]	S(1)-C(12)-C(15)	104 (4)
C(3)-Ir(2)-P(2)	93.6 (18)	S(2)-Ir(3)-C(5)	174.1[a]	C(13)-C(12)-C(14)	111 (4)
C(3)-Ir(2)-S(3)	105.1 (18)	S(3)-Ir(3)-C(4)	172.2[a]	C(13)-C(12)-C(15)	112 (4)
S(1)-Ir(2)-P(2)	169.7 (4)	S(3)-Ir(3)-C(5)	90.0[a]	C(14)-C(12)-C(15)	105 (4)
S(1)-Ir(2)-S(3)	90.7 (6)	C(4)-Ir(3)-C(5)	87.0[a]		

[a] Angles involving atoms in the rigid C(4)-C(5)-O(4)-O(5) group.

reveal any ketonic CO band in the 1700-cm^{-1} region, but they did show three terminal ν_{CO} bands. We propose that a rearrangement occurs in solution to give a new dinuclear complex **5'** bridged by two thiolato groups with two CO ligands in the equatorial positions and the third one in an axial position. When the IR spectra are started again the ν_{CO} band at 1913 cm^{-1} rapidly decreases and after about 10 min the only complex observed in solution was **2** characterized by 1956- and 1942-cm^{-1} ν_{CO} stretchings. Opening the IR cell gave a PMe_3 smell. The carbonylation of this solution restored (but not fully) complex **5'** with an excess of CO.

For complex **5'** the CO loss is too fast to record ^1H NMR spectra in solutions of C_6D_6 or $CDCl_3$, with complex **2** only being observed. Moreover, addition of 1 mol of PMe_2Ph ligand to complex **2**, $[Ir_2(\mu\text{-S-}t\text{-Bu})(CO)_2(PMe_3)_2]$, in toluene solution gave after a very quick carbonylation (1 min) the complex $[Ir_2(\mu\text{-S-t-Bu})_2(CO)_3(PMe_3)_2(PMe_2Ph)]$, which was characterized by IR (1957, 1940, and 1913 cm^{-1} in hexadecane). The same observation is made by adding 1 mol of PMe_3 under a CO atmosphere. Any attempt to crystallize these complexes failed, and in any case the complex of type **2** was obtained. We did not succeed in obtaining clear ^1H NMR spectra in benzene by starting from **2** and adding 1 mol of PMe_3 or PMe_2Ph under CO.

Moreover, analysis of complex **5** by mass spectrometry gave the parent ion of complex **2**. In this case too, the CO and PMe_3 losses are so fast that disubstituted complex **2** is observed.

Infrared spectra of complex **6** in CsBr pellets gave five ν_{CO} bands (Table XIII). The two bands at 2038 and 1976 cm^{-1} can reasonably be attributed to the CO ligands borne by the iridium(I) atom. Those at 1964 and 1947 cm^{-1} are related to the dinuclear entity, and the 1748 ν_{CO} band is attributed to the bridging CO group. Figure 5 shows the infrared spectra obtained for freshly prepared hexadecane solutions of **6**. Except for the 1748-cm^{-1} band of **6**, no ketonic band was detected. As for **5**, the CO loss was very fast and was found to be necessary to record the spectra as quickly as possible. When the ν_{CO} bands due to **6** decreased, seven new ν_{CO} bands appeared and were attributed to complexes **1**, **2**, and **3**. In a previous study[4] we have shown that equimolecular mixtures of **1** and **2** gave, after equilibrium, a dynamical exchange process of **3** between **1** and **2**. In the present case the CO loss was followed by the splitting of the trinuclear entity, giving the complexes **3** and **2**. Presumably as soon as it is formed complex **3** is in equilibrium with complexes **1** and **2**. This CO loss occurs very rapidly in solution so that after about 5 min no more complex **6** was observed and the IR spectra were the same as those obtained when complexes **1** and **2** are mixed in the ratio 1:2.[4] Mass spectrometry of complex **6** gave by electron impact the parent ion of complex **3**, $[Ir_2(\mu\text{-S-}t\text{-Bu})_2(CO)_3PMe_3]$. We were unable to detect the fragmentation peaks of complex **6** even by using the field-desorption techniques. This result gives further evidence for the breaking of the trinuclear molecule to give complex **3**.

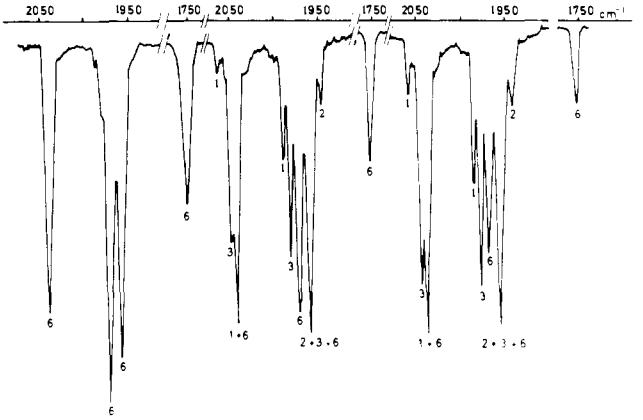

Figure 5. Sketch of three IR spectra in the ν_{CO} region taken as quickly as possible when $[Ir_3(\mu\text{-CO})(\mu\text{-S-}t\text{-Bu})_3(CO)_4(PMe_3)_2]$ (**6**) is dissolved in hexadecane. See text for labeled bands.

Discussion

The information obtained from the two structures in the solid state and from the study of the CO loss in solution allows further insight into the intermediates present in solution during the substitution of CO by phosphine ligands to be gained. Indeed the experiments were performed specifically with very small Schlenk tubes in order to avoid extended CO loss. We proposed Scheme II to rationalize our observations.

The major feature is that during the substitution process (**1** → **7** → **8** or **8'** → **9**) one of the two bridges is broken leading to two square planes attached by the remaining SR bridging group (**9**). After rearrangement of the square pyramid through a classical SP–TBP–SP interconversion,[28,29] complex **10** is obtained which loses a CO ligand and gives complex **11** with a CO-bridging ligand. It seems to us that complex **11** is the *key intermediate* since it contains already two phosphine ligands in the equatorial positions and a CO ligand in one of the two axial positions. This hypothesis is enhanced by the fact that further addition of stabilizing ligands such as PMe_3 or "$RSIr(CO)_2$" moiety (vide infra) leads to complexes **5** and **6** of fully characterized geometry. Let us mention that in diluted solutions, for example 0.01 M instead of 0.1 M of **1**, disubstituted complex **2** is obtained instead of **7**. The unexpected "$RS\,Ir\,(CO)_2$" ligand mentioned in Scheme II either is of very short life time or is obtained by breaking of the tetracarbonyl complex **1** after association to **10**. Another alternative seems unlikely since if the undercoordinated $RS\text{-}Ir(CO)_2$ species

(28) Jesson, J. P.; Meakin, P. *J. Am. Chem. Soc.* **1973**, *95*, 1344–1346.
(29) Shapley, J. R.; Osborn, J. A. *Acc. Chem. Res.* **1973**, *6*, 305–312.

Scheme II

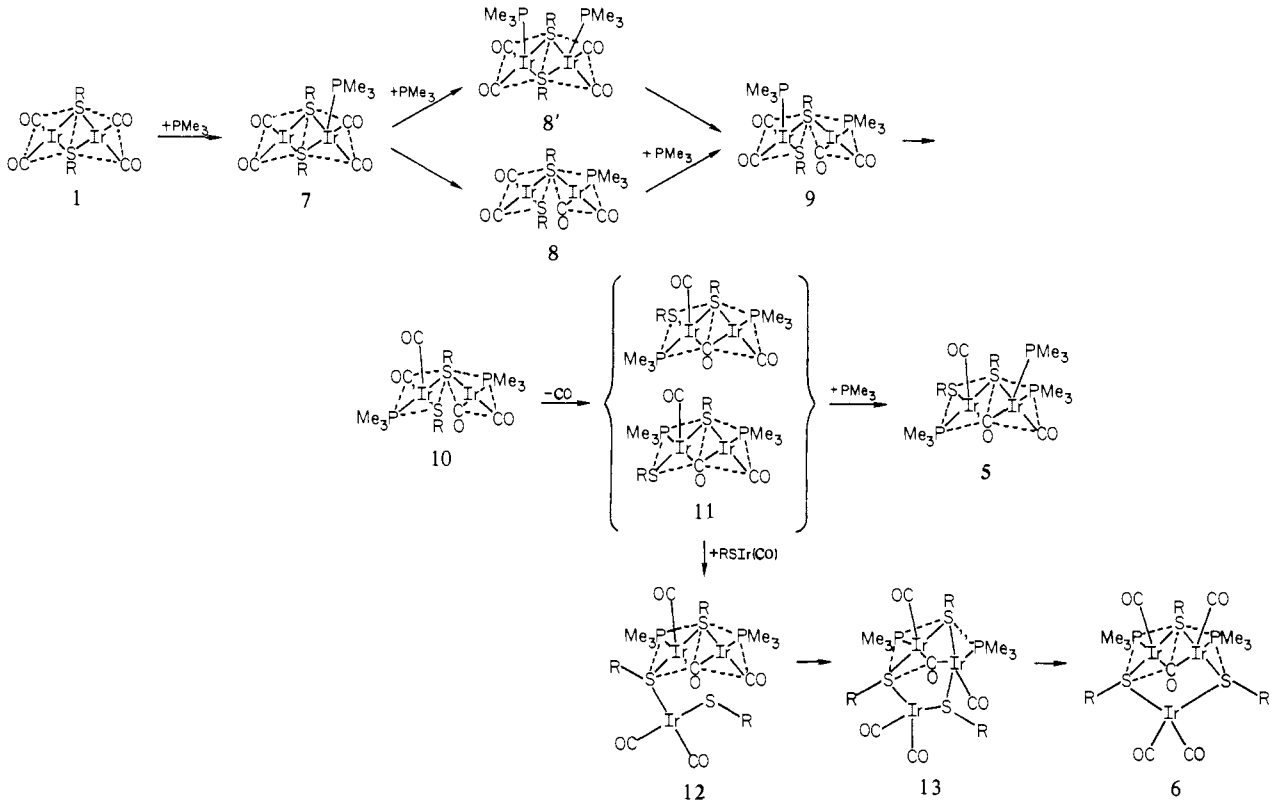

existed it would react very rapidly with the PMe_3 ligand to form the analogue of Vaska's complex[30,31] [RS Ir(CO)$(PMe_3)_2$], which was not detected.

In the case of rhodium chemistry, prior to the substitution process, the adduct with two phosphine ligands, [$Rh_2(\mu$-S-*t*-Bu$)_2(CO)_4L_2$], was observed (see **8'**). From infrared and ^1H NMR data ligands L were assigned in the apical positions of two square pyramids.[2] When L = PCy_3 the complex is less reactive than in those cases where there are other phosphorus ligands and a trace amount of a yellow solid is isolated. The IR spectrum of this solid phase is identical with that in a solution failing to reveal the presence of a CO-bridging ligand. It is difficult to prefer a priori one of the two pathways **7** → **8** → **9** or **7** → **8'** → **9**. At least it is easy to admit that the path **8'** → **2** would be prefered for rhodium complexes to the path **8'** → **9** presumably followed by iridium complexes. Concerning the capture of the CO group in step **10** → **11**, it seems to us that the presence of more diffuse orbitals on the iridium atoms can be involved.

Moreover, in complexes **5** and **6** under investigation the ν_{CO} stretching bands for the bridging CO are quite low, especially for complex **5**, i.e., 1703 cm^{-1} (see Table XIV). Such a value is no longer unexpected, since similar values have been observed for various rhodium,[19,22,23] iridium,[15] palladium,[20] and platinum[21] neutral complexes. In the case of [$Pd_2Cl_2(\mu$-CO)$(\mu$-$Ph_2AsCH_2AsPH_2)_2$][20] and [$Pt_2Cl_2(\mu$-CO)$(\mu$-$Ph_2AsCH_2AsPh_2)_2$],[21] as pointed out by Robinson[32] and Brown et al.,[21] the complexes may be formulated as dimetalated ketones due to the angles of ca. 120° around the carbon atom and the low ν_{CO} values of ca. 1700 cm^{-1}. However, for complexes [$Rh_2Br_2(\mu$-CO)-$(Ph_2PCH_2PPh_2)_2$][22] and [$Rh_2Cl_2(\mu$-CO)$(\mu$-$C_6H_6O_4$)-$(Ph_2PCH_2PPh_2)_2$][23] the term ketonic carbonyl ligand has been used to designate a carbonyl group which bridges the two metal centers either in the first complex with the Rh–Rh distance of 2.7566 (9) Å (both Rh–C–O angles are equal to 135.3 (6)° and the Rh–C–Rh angle is 89.4 (4)°) or in the second complex with the distance of 3.3542 (9) Å (both Rh–C–O angles are 122.0 (2) Å and the Rh–C–Rh angle is 116.0 (4)°). For the two complexes the CO stretching bands for the bridging CO ligands are 1745- and 1700-cm^{-1}, respectively.

Table XIV. Infrared Data for the Complexes **1**–**6** (ν_{CO} Region)

	CsBr	hexadecane
1 [$Ir_2(\mu$-S-*t*-Bu$)_2(CO)_4$]		2061 (s)
		2040 (vs)
		1986 (vs)
3 [$Ir_2(\mu$-S-*t*-Bu$)_2(CO)_3(PMe_3)$]		2046 (vs)
		1979 (vs)
		1957 (vs)
2 [$Ir_2(\mu$-S-*t*-Bu$)_2(CO)_2(PMe_3)_2$]	1941 (vs)	1956 (vs)
	1927 (vs)	1942 (vs)
5 [$Ir_2(\mu$-CO)$(\mu$-S-*t*-Bu$)(CO)_2$(S-*t*-Bu)-$(PMe_3)_3$]	1951 (s)	1957 (vs)
	1941 (vs)	1941 (s)
	1703 (vs)	1913 (s)
6 [$Ir_3(\mu$-S-*t*-Bu$)_3(\mu$-CO$)(CO)_4(PMe_3)_2$]	2038 (s)	2038 (s)
	1976 (s)	1969 (vs)
	1964 (vs)	1956 (s)
	1947 (vs)	1756 (m)
	1748 (s)	
4 [$Rh_2(\mu$-S-*t*-Bu$)_2(CO)_4(PCy_3)_2$][2]	2049 (vs)	2052
	1984 (s)	1989
	1952 (vs)	1956

For complexes **5** and **6** in the present study we have interpreted the short iridium–iridum separation in terms of a metal–metal bond. We believe that in fact they are not two quite different situations as proposed by Robinson,[32] who distinguishes between the keto bridge (M–C–M bond angle of ca. 120° and a ν_{CO} value of ca. 1700 cm^{-1}) and the classical CO bridge characterized by a M–C–M angle of 80–85° and a ν_{CO} value of ca. 1850 cm^{-1}. Such a clear-cut distinction cannot account for a good description of complexes **5**, **6**, and [$Rh_2Br_2(\mu$-CO$)(Ph_2PCH_2PPh_2)_2$].[22] Moreover, from the ν_{CO} frequency no univocal conclusion can be made for the M–M distance since it is 2.7 Å with a ν_{CO} stretching frequency of 1703 and 1748 cm^{-1} in **5** and **6** respectively, whereas with ν_{CO} in the same region, i.e., 1720 cm^{-1}, in [$Pd_2Cl_2(\mu$-CO$)(\mu$-$Ph_2AsCH_2AsPh_2)$] the M–M separation is much more longer, i.e., 3.274 (8) Å.[20]

(30) Vaska, L.; Di Luzio, J. W. *J. Am. Chem. Soc.* **1961**, *83*, 2784–2784.
(31) Gaines, T.; Roundhill, D. M. *Inorg. Chem.* **1974**, *13*, 2421–2522.
(32) Robinson, S. D. *Inorg. Chim. Acta* **1978**, *27*, L108–L108.

A large metal-metal distance, i.e., greater than 3 Å, supported by a bridging CO leads to a clear situation that can be described as a dimetalated ketone.[32] A CO group bonding two metal centers with a short distance can now be regarded as either a distorted dimetalated ketone or a two-electron-donor bridging group between two bonded metal centers.

Braterman[33] has already argued against the idea of ketonic carbonyl groups in favor of a delocalized molecule orbital description. Colton and McCormick[34] have suggested that it makes no difference whether spin pairing occurs via bridging carbonyl groups or via π interactions between the metals. Finally a general description for the M-C(O)-M moiety can be, to our opinion, formulated in any case as a three-center, four-electron bond.

(33) Braterman, P. S. *Struct. Bonding (Berlin)* **1972**, *10*, 57.
(34) Colton, R.; Mc Cormick, M. J. *Coord. Chem. Rev.* **1980**, *31*, 1-52.

Registry No. 1, 63312-27-6; **2**, 63292-79-5; **3**, 81219-06-9; **5**, 81219-07-0; **6**, 81219-08-1.

Supplementary Material Available: Tables of observed and calculated structure factors for **5** and **6** (Tables III and VII) and root-mean-square components of thermal displacement along principal axis for **5** and **6** (Table IV and VIII) (24 pages). Ordering information is given on any current masthead page.

Preparation of Organoimido and μ-Dinitrogen Complexes of Tantalum and Niobium from Neopentylidene Complexes

Scott M. Rocklage and Richard R. Schrock*

Contribution from the Department of Chemistry, Massachusetts Institute of Technology, Cambridge, Massachusetts 02139. *Received October 13, 1981*

Abstract: $M(CHCMe_3)(THF)_2X_3$ reacts with RN=CHPh (M = Ta, Nb; X = Cl, Br; R = Ph, CMe_3, Me) to give organoimido complexes $M(NR)(THF)_2Cl_3$ and $Me_3CCH{=}CHPh$ quantitatively. The THF ligands can be displaced by phosphines to give complexes such as *cis,mer*-$Ta(NR)(PMe_3)_2Cl_3$. The $Ta(NR)L_2Cl_3$ complexes (L = PMe_3, 0.5dmpe) can be reduced in the presence of L to give the Ta(III) complexes $Ta(NR)L_4Cl$ in high yield, and these, in turn, react with ethylene or styrene to give olefin complexes $Ta(NPh)(olefin)L_3Cl$. Several ^{15}N-labeled phenylimido compounds have been prepared and examined by ^{15}N NMR and IR ($\delta(^{15}NR)$ = 300-350 vs. NH_3, $\nu_{TaNR} \approx 1350$ cm^{-1}). The products of the reaction between $M(CHCMe_3)(THF)_2Cl_3$ and $PhCH{=}NN{=}CHPh$ are $[MCl_3(THF)_2]_2(\mu\text{-}N_2)$ and 2 equiv of $Me_3CCH{=}CHPh$. Phosphine complexes such as $[TaCl_3(PEt_3)_2]_2(\mu\text{-}N_2)$ can be prepared straightforwardly from the THF complexes. The organoimido complexes react with benzaldehyde to give RN=CHPh in high yield. The $\mu\text{-}N_2$ complexes react with acetone to give $Me_2C{=}NN{=}CMe_2$ and with HCl to give $N_2H_4{\cdot}2HCl$ in high yield.

Niobium and tantalum alkylidene complexes have been studied in our group for several years.[1] We have recently found that one of the simplest, $M(CHCMe_3)(THF)_2Cl_3$,[2] reacts with internal olefins to give several turnovers of metathesis products.[3] Therefore we became interested in the possibility of developing a metathesis-like reaction of imines with these alkylidene complexes to prepare simple alkylimido analogues, $M(NR)(THF)_2Cl_3$. After this initial success,[4] it became apparent that a metathesis-like reaction between $M(CHCMe_3)(THF)_2Cl_3$ and $PhCH{=}NN{=}CHPh$ could lead to molecules having an M=NN=M linkage; i.e., μ-dinitrogen complexes. In this paper we discuss the synthesis, characterization, and a few reactions of alkylimido and μ-dinitrogen complexes prepared by metathesis-like reactions. Simplicity and high yields made these unique routes attractive as entries into alkylimido[4] and μ-dinitrogen[5] chemistry of niobium and tantalum.

Results

When RN=CHPh is added to $M(CHCMe_3)(THF)_2X_3$ in ether, cis- and trans-$Me_3CCH{=}CHPh$ and the yellow (R = Ph) or white (R = Me or CMe_3) imido complexes form quantitatively (eq 1). When PhN=CHPh is added to $M(CHCMe_3)(THF)_2X_3$,

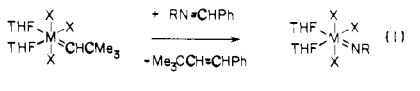

M = Nb, Ta, X = Cl, Br, R = Ph, CMe_3, Me

the reaction is complete in 1 h. However, when $PhN{=}CHCMe_3$ is used, the reaction takes 18-20 h, and when $Me_3CN{=}CHCMe_3$ is used, no reaction is observed after 24 h at 25 °C. These results can all be explained by steric considerations in an intermediate containing an MC_2N ring (eq 2). The cis,mer configuration for

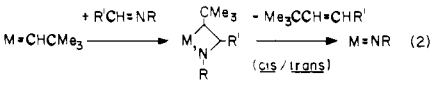

$M(NR)(THF)_2X_3$ is proposed on the basis of the presence of two types of THF ligands in the ^1H NMR spectra. When THF is added to the sample, the signals for coordinated THF are broadened due to exchange of the free THF with the coordinated THF.

The reaction between $Ta(NR)(THF)_2X_3$ and PMe_3 gives light yellow $Ta(NR)(PMe_3)_2Cl_3$ (eq 3). The cis,mer configuration

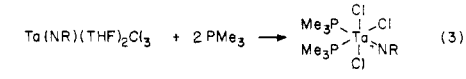

is proposed since the PMe_3 ligands are inequivalent (-11.65 and -40.0 ppm in the $^{31}P\{^1H\}$ NMR spectrum at -30 °C) and one of them (we propose the PMe_3 ligand trans to the imido ligand at

(1) Schrock, R. R. *Acc. Chem. Res.* **1979**, *12*, 98-104.
(2) Rupprecht, G. A.; Messerle, L. W.; Fellmann, J. D.; Schrock, R. R. *J. Am. Chem. Soc.* **1980**, *102*, 6236-6244.
(3) Rocklage, S. M.; Fellmann, J. D.; Rupprecht, G. A.; Messerle, L. W.; Schrock, R. R. *J. Am. Chem. Soc.* **1981**, *103*, 1440-1447.
(4) Rocklage, S. M.; Schrock, R. R. *J. Am. Chem. Soc.* **1980**, *102*, 7808-7809.
(5) Turner, H. W.; Fellmann, J. D.; Rocklage, S. M.; Schrock, R. R.; Churchill, M. R.; Wasserman, H. J. *J. Am. Chem. Soc.* **1980**, *102*, 7809-7811.

0002-7863/82/1504-3077$01.25/0 © 1982 American Chemical Society